

# Flight Attitude Control of an Electric Vertical Takeoff and Landing with Flexible Frame

Yu Zhang  
School of Mechanical Engineering,  
Beijing Institute of Technology,  
Beijing, China  
bitzhangyu2022@163.com

Wei Fan\*  
Chongqing Innovation Center, Beijing  
Institute of Technology, Chongqing,  
China  
fanweixx@bit.edu.cn

Bin Xu  
School of Mechanical Engineering,  
Beijing Institute of Technology,  
Beijing, China  
bitxubin@bit.edu.cn

Changle Xiang  
School of Mechanical Engineering,  
Beijing Institute of Technology,  
Beijing, China  
xiangcl@bit.edu.cn

Hua Zhu  
School of Mechanical Engineering,  
Beijing Institute of Technology,  
Beijing, China  
bitzhuhua@bit.edu.cn

Xing Yue  
Chongqing Innovation Center, Beijing  
Institute of Technology, Chongqing,  
China  
xingyue@bit.edu.cn

## ABSTRACT

The stability problem of an Electric Vertical Takeoff and Landing (eVTOL) aircraft with flexible frame is investigated in this paper. A spring damping model is adopted to describe the deformation of the frame of eVTOL, where modeling and parameter uncertainties are considered. Based on the L1 output feedback algorithm, an adaptive controller is proposed to augment the stability of the eVTOL system. Numerical simulation is conducted to illustrate the effectiveness and feasibility of the theoretical results.

## CCS CONCEPTS

• Computing methodologies; • Artificial intelligence; • Control methods; • Computational control theory;

## KEYWORDS

eVTOL, Flexible frame, Input error, Adaptive control

### ACM Reference Format:

Yu Zhang, Wei Fan\*, Bin Xu, Changle Xiang, Hua Zhu, and Xing Yue. 2021. Flight Attitude Control of an Electric Vertical Takeoff and Landing with Flexible Frame. In *The 5th International Conference on Computer Science and Application Engineering (CSAE 2021), October 19–21, 2021, Sanya, China*. ACM, New York, NY, USA, 6 pages. <https://doi.org/10.1145/3487075.3487126>

## 1 INTRODUCTION

Because of its good maneuverability and stability, eVTOL has gradually attracted extensive attention from international scholars [1]. Among them, four-rotor, six-rotor and other rotor configurations have been widely used in many fields, such as aerial photography [2], logistics [3], pesticide spraying [4] and high-altitude unmanned

reconnaissance [5], due to their advantages of simple structure, stability and reliability. However, research in the field of aircraft has focused on small eVTOL. With the development of unmanned flying technology, requirements for the carrying capacity of eVTOL become higher and higher. Therefore, large unmanned aerial vehicles such as EHANG 184 [6] and Joby Aviation's Joby S4 [7], which can realize heavy-duty or manned flight, have gradually become a hot research topic.

Compared to small eVTOL, large eVTOL need to be more in-depth researched in terms of the lifting load requirements, lightweight design, and structural rigidity. In [8] the authors designed and optimized the rotor airfoil from the perspective of aerodynamic optimization. Effects of stall delay and blade flexibility on performance are also studied. The blade structure was designed from the perspective of blade inertial and structural properties [9]. By using the method of comprehensive analysis, the performance was optimized in order to get the optimum twist, collective, tip speed, and taper. A novel design methodology was presented by Ong. W. et al. [10] for multirotor eVTOL to solve the problems in the design process of vehicles with heavy lifting capabilities. The coaxial rotor systems that exhibit the best thrust-to-volume ratio for eVTOL operation in an urban environment were included in their work to extend existing design methodologies.

At present, researches on large eVTOL mainly focused on optimization of the propeller based on aerodynamics and blade design, and the various indicators of eVTOL were achieved from the structural design. No analysis or research was conducted from the perspective of eVTOL frame deformation.

Concerned with the deformation of the eVTOL frame, the X-MORF Quadrotor provided a structure which was composed of two independent arms [11]. It changes the geometry of the drone by adjusting the angle between the arms. The Model Reference Adaptive Control (MRAC) was used to address the uncertainties about inertia and center of mass caused by the active deformation structure of the quadrotor. The results showed that the controller has good stability and attitude tracking performances. An eVTOL was designed in ref. [12], which uses a four-link mechanism with revolute flexible joints as a support frame. It achieved controllability and flexibility at the same time. When the eVTOL frame deformed due to the collision with external objects, it has good robustness merely by

Permission to make digital or hard copies of all or part of this work for personal or classroom use is granted without fee provided that copies are not made or distributed for profit or commercial advantage and that copies bear this notice and the full citation on the first page. Copyrights for components of this work owned by others than ACM must be honored. Abstracting with credit is permitted. To copy otherwise, or republish, to post on servers or to redistribute to lists, requires prior specific permission and/or a fee. Request permissions from [permissions@acm.org](mailto:permissions@acm.org).

CSAE 2021, October 19–21, 2021, Sanya, China

© 2021 Association for Computing Machinery.

ACM ISBN 978-1-4503-8985-3/21/10...\$15.00

<https://doi.org/10.1145/3487075.3487126>

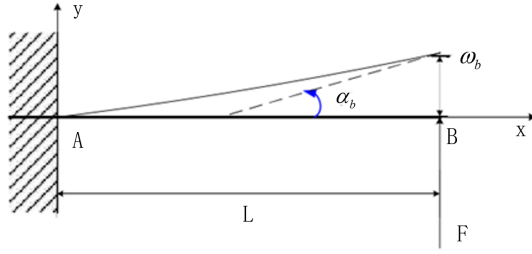


Figure 1: Force Deformation Diagram of a Single Arm.

the control of closed-loop PI. Harbin Institute of Technology in [13] had developed a miniature variable quadcopter that can be worn on the wrist. By simplifying the flexible frame to a cantilever beam, a dynamic model of the eVTOL was established. A PID controller has been designed to control attitude. The results showed that the controller can realize attitude tracking, but there is still room for improvement in tracking performance.

The large eVTOL with flexible frame generates deformation under the lifting force. The research of structural design may not be directly extended to a more general case. Furthermore, the traditional PID controllers do not suitable to control the attitude of eVTOL which possesses a flexible frame.

In this paper, in order to solve the problem of deformation of flexible frame eVTOL, we treat the flexible frame as a spring damping system to establish a dynamic model. And a controller based on the L1 adaptive algorithm is designed to control the flight attitude of the large eVTOL.

The main part of this paper is performed as follows. In section 2, the comprehensive nonlinear model of the eVTOL is established. In section 3, an output feedback L1 adaptive controller is designed. In section 4, the numerical experiments results and analysis of the proposed controller are carried out. Finally, some conclusions are drawn in section 5.

## 2 COMPREHENSIVE NONLINEAR MODELING

The vertical deformation of the frame will affect the flight stability according to the stress condition during the flight of large eVTOL. The comprehensive nonlinear model of the eVTOL is accomplished through equating the frame to a spring damping system as follows.

### 2.1 Modeling of a Single Arm

According to aerodynamics, the rotation of the propeller will generate lift force, which acts on the motor base. The torque force generated by propeller rotation is acted on the body. It doesn't matter with whether the frame is flexible or rigid. Therefore, the influence of lift on the flexible frame needs to be considered only. The mechanical model of the flexible frame can be approximated to the cantilever beam model to obtain the bending angle and deflection of the arm. As shown in Figure 1

$$\begin{cases} \alpha_b = FL^2 / 2EI \\ \omega_b = FL^3 / 3EI \end{cases} \quad (1)$$

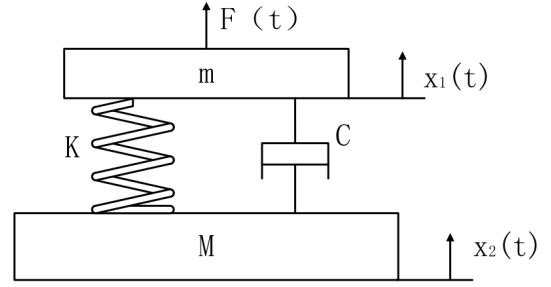


Figure 2: Spring Damping Vibration System.

Where  $F$  is the lift force of the propeller,  $L$  is the arm length,  $E$  is the flexural rigidity of the arm,  $\alpha_b$  is the bending angle,  $\omega_b$  is the deflection.

The flexible arm is not only concerned with the problem of force deformation, but vibration is also important. As shown in Figure 2, it is equivalent to a spring damping system. The mechanical vibration and deformation under force were combined to simulate the flexibility of the arm due to the short of rigid.

The force condition of the power unit is obtained:

$$m\ddot{x}_1(t) = F(t) - C[\dot{x}_1(t) - \dot{x}_2(t)] - K[x_1(t) - x_2(t)] - mg \quad (2)$$

Where  $m$  is the mass of the power unit,  $M$  is the body quality,  $K$  is the elastic coefficient,  $C$  is the damping coefficient,  $F(t)$  is the lift force produced by the power unit.

The force  $T(t)$  acts on the body is obtained:

$$T(t) = [C[\dot{x}_1(t) - \dot{x}_2(t)] - K[x_1(t) - x_2(t)]] \cdot \cos[F(t)L^2 / 2EI] \quad (3)$$

### 2.2 Modeling of the eVTOL with a Flexible Frame

The spring damping model of the eVTOL is shown in Figure 3. Where  $O_b - X_b Y_b Z_b$  is the body coordinate system,  $O_e - e_x e_y e_z$  is the earth coordinate system.

For the following derivation, table 1 shows the description of the parameters of the eVTOL.

According to Eq. 2), we can get:

$$\begin{cases} m\ddot{z}_{nb} = F_n - K(z_{nb} - z_b) - C(\dot{z}_{nb} - \dot{z}_b) - mg; \\ n = 1, 2, 3, 4 \end{cases} \quad (4)$$

The rotation matrix between the body coordinate system and the earth coordinate system can be derived as:

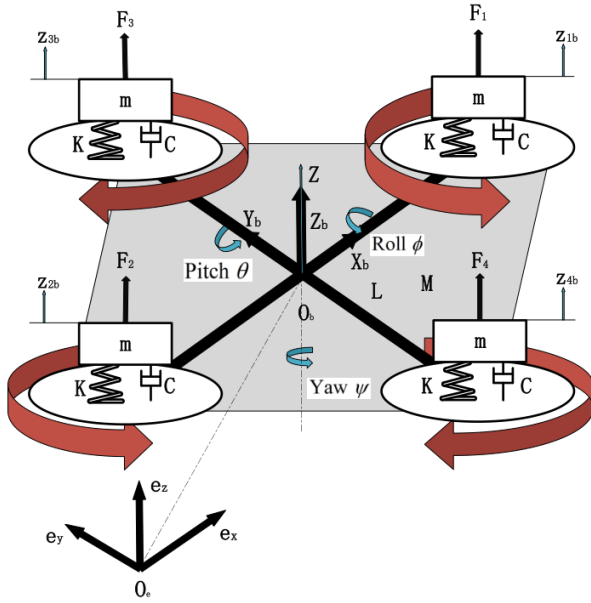
$$R = \begin{bmatrix} c_\psi c_\phi & c_\psi s_\theta s_\phi - c_\psi s_\phi & c_\psi s_\theta c_\phi + s_\psi s_\phi \\ s_\psi c_\theta & s_\psi s_\theta s_\phi + c_\psi s_\phi & c_\psi s_\theta c_\phi - s_\psi c_\phi \\ -s_\theta & c_\theta s_\phi & c_\theta c_\phi \end{bmatrix} \quad (5)$$

Where  $s_\Delta$  refers to  $\sin \Delta$  and  $c_\Delta$  refers to  $\cos \Delta$ . The force condition of the body is obtained:

$$\begin{cases} M \begin{bmatrix} \ddot{x}_e \\ \ddot{y}_e \\ \ddot{z}_e \end{bmatrix} = \sum_{n=1}^4 (K(z_{nb} - z_b) + C(\dot{z}_{nb} - \dot{z}_b)) R_3 \cos[F_n L^2 / 2EI] - \begin{bmatrix} 0 \\ 0 \\ Mg \end{bmatrix} - \begin{bmatrix} K_x \dot{x}_e \\ K_y \dot{y}_e \\ K_z \dot{z}_e \end{bmatrix} \\ R_3 = \begin{bmatrix} \cos \psi \sin \theta \cos \phi + \sin \psi \sin \phi \\ \cos \psi \sin \theta \cos \phi - \sin \psi \cos \phi \\ \cos \theta \cos \phi \end{bmatrix} \end{cases} \quad (6)$$

**Table 1: Description of Various Parameters of Drone**

Parameter	Physical description	unit
$\theta$	Pitch attitude angle	rad
$\phi$	Roll attitude angle	rad
$\psi$	Yaw attitude angle	rad
$F_n, n = 1, 2, 3, 4$	Lift generated by the power unit	N
$z_{nb}, n = 1, 2, 3, 4$	Displacement of the end of the arm in the z-axis direction	m
$z$	Displacement of the body in the z-axis direction	m
$m$	Power unit quality	kg
$M$	Body mass	kg
$K$	Coefficient of elasticity	/
$C$	Damping coefficient	/
$L$	Arm length	m

**Figure 3: Diagram of Equivalent Quadrotor Model.**

Where  $K_x, K_y, K_z$  are the coefficient of air resistance in the x-axis, y-axis, z-axis direction, respectively.

When the attitude angle is changed at a small increment, according to Euler's rotation equation, the resultant external moment of the eVTOL in the body coordinate system can be obtained as:

$$\begin{cases} M_x = I_x \ddot{\phi} + \dot{\theta} \dot{\psi} (I_z - I_y) \\ M_y = I_y \ddot{\theta} + \dot{\phi} \dot{\psi} (I_x - I_z) \\ M_z = I_z \ddot{\psi} + \dot{\phi} \dot{\theta} (I_y - I_x) \end{cases} \quad (7)$$

Where  $M_x, M_y, M_z$  are the total external moments in the x-axis, y-axis, and z-axis directions, respectively,  $I_x, I_y, I_z$  are the moments of inertia in the x-axis, y-axis, and z-axis directions respectively.

Since the eVTOL system is a complex under-actuated system with four inputs and six outputs, the four virtual control variables

are obtained:

$$\begin{cases} U_1 = \sum_{n=1}^4 ((K(z_{nb} - z_b) + C(\dot{z}_{nb} - \dot{z}_b)) \cos(F_n L^2 / 2EI)) \\ U_2 = (K(z_{2b} - z_b) + C(\dot{z}_{2b} - \dot{z}_b)) \cos(F_2 L^2 / 2EI) \\ \quad - (K(z_{1b} - z_b) + C(\dot{z}_{1b} - \dot{z}_b)) \cos(F_1 L^2 / 2EI) \\ U_3 = (K(z_{3b} - z_b) + C(\dot{z}_{3b} - \dot{z}_b)) \cos(F_3 L^2 / 2EI) \\ \quad - (K(z_{4b} - z_b) + C(\dot{z}_{4b} - \dot{z}_b)) \cos(F_4 L^2 / 2EI) \\ U_4 = B(\omega_1^2 + \omega_2^2 - \omega_3^2 - \omega_4^2) \end{cases} \quad (8)$$

Where  $U_1$  is the controlled amount of drone ascent,  $U_2$  is the control amount of the drone's pitch angle,  $U_3$  is the control amount of the drone's roll angle,  $U_4$  is the control amount of the drone's yaw angle,  $B$  is the anti-torque proportional coefficient of the motor,  $\omega_n$  ( $n = 1, 2, 3, 4$ ) is the speed of each motor.

Therefore, the dynamic equation of the flexible frame eVTOL is given as follows:

$$\begin{cases} \ddot{x}_e = \frac{\sum_{n=1}^4 ((K(z_{nb} - z_b) + C(\dot{z}_{nb} - \dot{z}_b)) \cos(F_n L^2 / 2EI)) \cdot \cos \psi \sin \theta \cos \phi + \sin \psi \sin \phi}{M} \\ \ddot{y}_e = \frac{\sum_{n=1}^4 ((K(z_{nb} - z_b) + C(\dot{z}_{nb} - \dot{z}_b)) \cos(F_n L^2 / 2EI)) \cdot \cos \psi \sin \theta \cos \phi - \sin \psi \cos \phi}{M} \\ \ddot{z}_e = \frac{\sum_{n=1}^4 ((K(z_{nb} - z_b) + C(\dot{z}_{nb} - \dot{z}_b)) \cos(F_n L^2 / 2EI)) \cdot \cos \theta \cos \phi - g}{M} \\ \ddot{z}_{nb} = \frac{F_n - K(z_{nb} - z_b) - C(\dot{z}_{nb} - \dot{z}_b)}{m} - g, n = 1, 2, 3, 4 \\ \ddot{\phi} = \frac{\dot{\theta} \dot{\psi} (I_z - I_y)}{I_x} - \frac{L((K(z_{2b} - z_b) + C(\dot{z}_{2b} - \dot{z}_b)) \cos(F_2 L^2 / 2EI))}{I_x} \\ \quad + \frac{(K(z_{1b} - z_b) + C(\dot{z}_{1b} - \dot{z}_b)) \cos(F_1 L^2 / 2EI)}{I_x} \\ \ddot{\theta} = \frac{\dot{\phi} \dot{\psi} (I_x - I_z)}{I_y} - \frac{L((K(z_{3b} - z_b) + C(\dot{z}_{3b} - \dot{z}_b)) \cos(F_3 L^2 / 2EI))}{I_y} \\ \quad + \frac{(K(z_{4b} - z_b) + C(\dot{z}_{4b} - \dot{z}_b)) \cos(F_4 L^2 / 2EI)}{I_y} \\ \ddot{\psi} = \frac{\dot{\phi} \dot{\theta} (I_y - I_x) - LB(\omega_1^2 + \omega_2^2 - \omega_3^2 - \omega_4^2)}{I_z} \end{cases} \quad (9)$$

### 3 ATTITUDE CONTROLLER DESIGN

Through the uncertainty analysis of the flexible frame eVTOL system, the design of the controller is shown as follows.

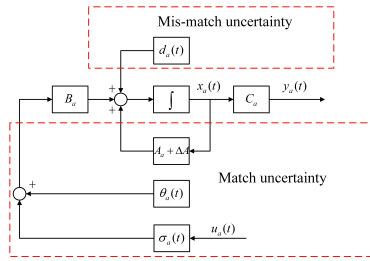


Figure 4: Schematic Diagram of System Uncertainty Structure.

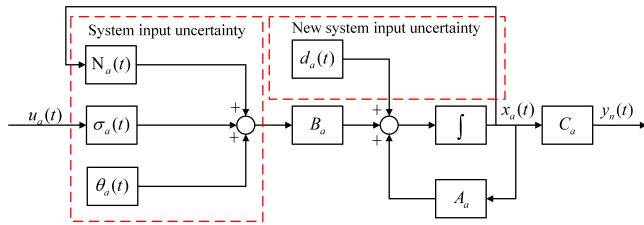


Figure 5: Uncertainty Analysis Diagram for Controller Design.

### 3.1 Uncertainty Analysis for Controller Design

The uncertainty of flexible frame eVTOL is comprised by matching uncertainty and mismatching uncertainty. Matching uncertainty mainly includes dynamic modeling error, system parameter error, and system input error. The mismatching uncertainty is mainly performed as the external disturbance of the system. Figure 4 shows a schematic diagram of the two uncertainties in the system.

The flexible frame eVTOL model with uncertainty can be expressed as:

$$\begin{cases} \dot{x}_a(t) = (A_a + \Delta A)x_a(t) + B_a(\sigma_a(t)u_a(t) + \theta_a(t)) + d_a(t) \\ y_a(t) = C_a x_a(t) \end{cases} \quad (10)$$

Where  $\Delta A$  is the system modeling and parameter error;  $\sigma_a(t)$  is the system input error;  $\theta_a(t)$  is the system identification error,  $d_a(t)$  is the external disturbance of the system.

Through mathematical derivation, the system state parameter error is converted to the system input error. The system disturbance is considered as the input of new system.

$$\begin{cases} \dot{x}_a(t) = A_a x_a(t) + B_a(\sigma_a(t)u_a(t) + N_a(t)x_a(t) + \theta_a(t)) + d_a(t) \\ y_a(t) = C_a x_a(t) \end{cases} \quad (11)$$

Where  $\Delta A = B_a N_a(t)$ .

A controller system model with uncertainties is obtained, as shown in Figure 5

This article mainly focuses on the research about the flexibility of the eVTOL frame, so the mismatching uncertainty is not considered in the controller design process.

So the system model is gotten as follow:

$$\begin{cases} \dot{x}_a(t) = A_a x_a(t) + B_a(\sigma_a(t)u_a(t) + N_a(t)x_a(t) + \theta_a(t)) \\ y_a(t) = C_a x_a(t) \end{cases} \quad (12)$$

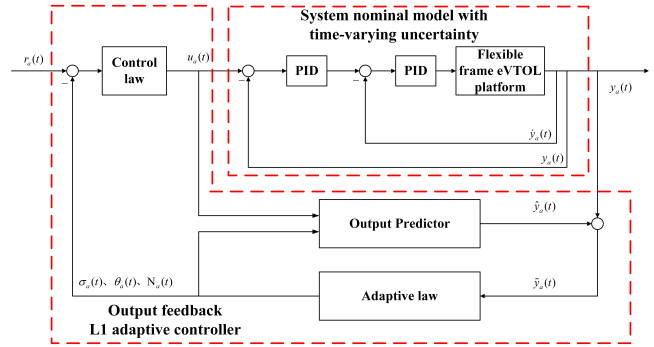


Figure 6: Schematic Diagram of the Control Model of the Flexible Frame eVTOL.

### 3.2 Attitude Controller Design Based on L1 Adaptive Algorithm

Based on the results of uncertainty analysis, the main uncertainty contained in the flexible frame eVTOL model is the system input error. This section will design a controller based on the L1 adaptive output feedback control algorithm.

As shown in Figure 6, the control system of this article is divided into two parts. The inner loop is a time-varying uncertainty nominal system which adapted the PID controller, and the outer loop is an output feedback controller based on the L1 adaptive control algorithm. The control problem of the flight attitude of the flexible frame eVTOL is mainly reflected in the control of pitch or roll channel (the two channels are similar), and it does not include the control of yaw channel. So in this section, a single input single output (SISO) control system is designed.

Consider closed-loop system:

$$y_a(s) = G_n(s)(u_a(s) + E_a(s)) \quad (13)$$

Where  $u_a(s)$  is the Laplace transform of the system's input signal  $u_a(t)$ ;  $y_a(s)$  is the Laplace transform of the system's output signal  $y_a(t)$ ;  $G_n(s)$  is a single channel transfer function of the nominal system of the inner loop;  $E_a(s)$  represents the system input error  $N_a(t) x_a(t)$ ,  $\theta_a(t)$  in the nominal system.

According to Lipschitz continuity condition, we can get continuity assumption of system uncertainty. There exist constants  $L_i > 0$  and  $L_0 > 0$ , such that:

$$\begin{cases} |f(t, y_1) - f(t, y_2)| \leq L |y_1 - y_2| \\ |f(t, y)| \leq L |y| + L_0 \end{cases} \quad (14)$$

Where  $f$  is an unknown map;  $f(t, y)$  is the time-varying nonlinear uncertainties and disturbances.

**3.2.1 Output Predictor.** Defining  $r_a(t)$  as a given bounded continuous reference input signal. The control objective is to design an adaptive output feedback controller  $u_a(t)$  in order that the system output  $y_a(t)$  tracks the reference input  $r_a(t)$  according to the required reference model  $G_M(s)$ .

From Eq. 13), we can get:

$$\begin{cases} y(s) = G_M(s)(u_a(s) + E_r(s)), y(0) = 0 \\ E_r(s) = \frac{(G_n(s) - G_M(s))u_a(s) + G_n(s)E_a(s)}{G_M(s)} \end{cases} \quad (15)$$

Eq. 15) is rewritten into the standard state space form:

$$\begin{cases} \dot{x}(t) = A_M x(t) + B_M(u_a(t) + E_r(t)) \\ y(t) = C_M x(t) \end{cases} \quad (16)$$

Where  $(A_M, B_M, C_M)$  is a minimal realization of  $G_M$ . For the closed-loop system given by Eq. 16), we can get the output predictor:

$$\begin{cases} \dot{\hat{x}}(t) = A_M \hat{x}(t) + B_M(u_a(t) + \hat{E}_r(t)) \\ \hat{y}(t) = C_M \hat{x}(t) \end{cases} \quad (17)$$

**3.2.2 Adaptation Law.**  $A_M$  is a Hurwitz matrix. According to the theory set forth in article[14] and its algebraic Lyapunov equation:

$$\begin{cases} \exists Q_M = Q_M^T \in R^{n_M \times n_M} \\ A_M^T Q_M + Q_M A_M = -I_{n_M \times n_M} \end{cases} \quad (18)$$

Where  $n_M$  is the order of the reference system  $A_M$ .

$$\begin{cases} \Lambda_M = \begin{bmatrix} C_M \\ T_M \sqrt{Q_M} \end{bmatrix} \\ T_M \left( \frac{C_M}{\sqrt{Q_M}} \right)^T = 0 \end{cases} \quad (19)$$

Where the real matrix  $\Lambda_M \in R^{n_M \times n_M}$ , the real matrix  $T_M$  is the null space of  $(C_M/\sqrt{Q_M})^T$ .

Define the error between the predicted value and the measured value as:

$$\tilde{y}(t) = \hat{y}(t) - y(t) \quad (20)$$

Based on Eq. 18) (19) (20), we get the adaptation laws:

$$\begin{cases} \hat{E}_r(t) = \hat{E}_r(iT_s), t \in [iT_s, (i+1)T_s] \\ \hat{E}_r(iT_s) = -\Phi^{-1}(T_s) u_r(iT_s), i = 0, 1, 2, \dots \\ \Phi(T_s) = \int_0^{T_s} e^{\Lambda_M A_M \Lambda_M^{-1}(T_s-t)} \Lambda_M dt \\ u_r(iT_s) = e^{\Lambda_M A_M \Lambda_M^{-1} T_s} \tilde{y}(iT_s) \end{cases} \quad (21)$$

**3.2.3 Control Law.** Based on Eq. 19) (21), the control signal is defined as:

$$u_a(s) = C(s) r_a(s) - \frac{C(s)}{C_M (sI_{n_M \times n_M} - A_M)^{-1} B_M} C_M (sI_{n_M \times n_M} - A_M)^{-1} \hat{E}_r(s) \quad (22)$$

Where  $C(s)$  is the low pass filter, according to the theory proposed in article[15], it follows the rules as listed:

$$\begin{cases} G_c(s) = \frac{G_n(s) G_M(s)}{C(s) G_n(s) + (I_{n_M \times n_M} - C(s)) G_M(s)} \\ \|G_c(s)(1 - C(s))\|_{L_1} < 1 \end{cases} \quad (23)$$

Where  $\|*\|_{L_1}$  represents the L1-norm of the corresponding system,  $L = [L_1, L_2, \dots, L_3]^T$  is the set vector of the constant  $L$  in the continuity assumption of the system uncertainty described by Eq. 14).

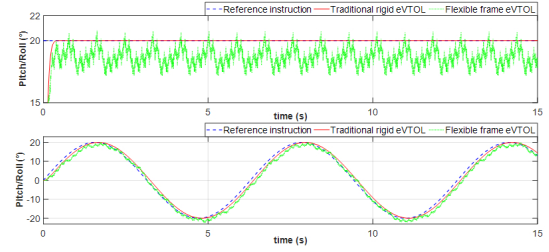


**Figure 7: The Attitude Response of the Rigid Frame and the Flexible Frame under the Control of Traditional PID Controller.**

So far, the L1 adaptive output feedback controller of the nominal closed-loop system is shown as follow:

$$\begin{cases} \begin{cases} \hat{x}(t) = A_M \hat{x}(t) + B_M (u_a(t) + \hat{E}_r(t)) \\ \hat{y}(t) = C_M \hat{x}(t) \end{cases} \\ \begin{cases} \hat{E}_r(t) = \hat{E}_r(iT_s), t \in [iT_s, (i+1)T_s] \\ \hat{E}_r(iT_s) = -\Phi^{-1}(T_s) u_r(iT_s), i = 0, 1, 2, \dots \\ \Phi(T_s) = \int_0^{T_s} e^{\Lambda_M A_M \Lambda_M^{-1}(T_s-t)} \Lambda_M dt \\ u_r(iT_s) = e^{\Lambda_M A_M \Lambda_M^{-1} T_s} \tilde{y}(iT_s) \\ u_a(s) = C(s) r_a(s) \end{cases} \\ - \frac{C(s)}{C_M (sI_{n_M \times n_M} - A_M)^{-1} B_M} C_M (sI_{n_M \times n_M} - A_M)^{-1} \hat{E}_r(s) \end{cases} \quad (24)$$

## 4 SIMULATION VERIFICATION AND ANALYSIS

In this section, we adopted the traditional PID controller to carry out control simulation of the rigid-body and the flexible frame eVTOL respectively, and the simulation of the flexible frame eVTOL controlled by L1 adaptive output feedback controller is conducted as well. The simulation results are compared and analyzed. As mentioned above, the simulation results showed the response of the pitch/roll channel only.

### 4.1 The Attitude Control of the Frame Flexible eVTOL by PID Controller

As shown in Figure 7, the traditional PID controller is adopted, and the reference signals are 20 degree step signal and sinusoidal signal respectively. The adjustment time of response curve of the rigid frame is less than 2 seconds. There is no overshoot and no steady-state error. It has good tracking performance in this condition. But, the response curve of the flexible frame oscillates near the reference curve, the adjustment time is relatively large, and there are overshoot and steady-state errors. The tracking performance is obviously relatively poor.

So the traditional PID controller has poor performance on controlling of the eVTOL with a flexible frame, and we need a more advanced controller.

### 4.2 Control Effect of L1 Adaptive Controller

As shown in Figure 7, when the system includes dynamic modeling error and system parameter errors, the traditional PID controller

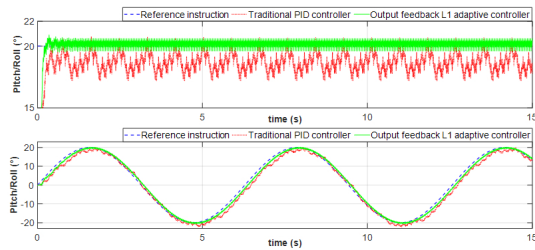


**Figure 8: The Attitude Response of the Flexible Frame under the Traditional PID Controller and the L1 Adaptive Output Feedback Controller.**

can track the reference signal, but the response curve has obvious oscillation, and the oscillation amplitude is in the range of 10%-20% compared with the reference signal. There are obvious steady-state errors. The L1 adaptive output feedback controller can track the reference signal. Compared with the traditional PID controller, the oscillation amplitude is less than 5%, and adjustment time is obviously reduced. The steady-state errors are eliminated. And the tracking effect is obviously improved.

Therefore, The L1 adaptive output feedback controller is more suitable for controlling the eVTOL with a flexible frame.

## 5 CONCLUSION

In this paper, a dynamic model was constructed to describe the dynamics of the eVTOL by treating the flexible frame as a spring damping system, and modeling error and parameter error of the eVTOL were considered. On the basis of the proposed dynamic model, the L1 adaptive output feedback controller was designed to stabilize the eVTOL subject to flexible frame. Simulation results showed that compared to the traditional PID controller, our proposed controller gained advantages in terms of eliminating the steady-state error, attenuating the oscillation amplitude and significantly reducing the adjustment time.

## ACKNOWLEDGMENTS

This study was co-supported by the National Natural Science Foundation of Chongqing, China(No. cstc2020jcyj-msxm3857) and National Key Research and Development Program of China (No. 2020YFC1512500). We also thank Beijing Institute of Technology for providing equipment and convenience for our work.

## REFERENCES

- [1] Zhang Y, Zeng Q, Wei Z (2017). Overview of UAV Development[J]. Henan Science and Technology.
- [2] Puttock A K, Cunliffe A M, Anderson K, *et al.* (2015). Aerial photography collected with a multirotor drone reveals impact of Eurasian beaver reintroduction on ecosystem structure[J]. Journal of Unmanned Vehicle Systems, 150429143447007.
- [3] Moshref-Javadi M, Winkenbach M (2021). Applications and Research Avenues for Drone-Based Models in Logistics: A Classification and Review[J]. Expert Systems with Applications, 114854.
- [4] Rafal, Perz, Kacper (2019). UAV application for precision agriculture[J]. Aircraft Engineering & Aerospace Technology.
- [5] Guo F, Zhang A, Zhang Y, *et al.* (2009). Numerically simulating survivability of high-altitude unmanned reconnaissance aerial vehicle (URAV)[J]. Journal of Northwestern Polytechnical University, 27(6):827-832.
- [6] Tilley, Aaron (2016). Chinese Drone Maker EHang Announces An Autonomous Flying Vehicle For People.[J]. Forbes.com, 6-6.
- [7] Pólaczyk N, Trombino E, Wei P, *et al.* (2019). A review of current technology and research in urban on-demand air mobility applications[C]//8th Biennial Autonomous VTOL Technical Meeting and 6th Annual Electric VTOL Symposium.
- [8] Acree Jr C W, Martin P B, Romander E A (2006). Impact of Airfoils on Aerodynamic Optimization of Heavy Lift Rotorcraft[R]. NATIONAL AERONAUTICS AND SPACE ADMINISTRATION MOFFETT FIELD CA AMES RESEARCH CENTER.
- [9] Yeo H, Johnson W (2007). Aeromechanics analysis of a heavy lift slowed-rotor compound helicopter[J]. Journal of Aircraft, 44(2): 501-508.
- [10] Ong W, Srigrarom S, Hesse H (2019). Design methodology for heavy-lift unmanned aerial vehicles with coaxial rotors[C]//AIAA Scitech 2019 Forum, 2095.
- [11] Desbiez A, Expert F, Boyron M, *et al.* (2017). X-Morf: A crash-separable quadrotor that morphs its X-geometry in flight[C]//2017 Workshop on Research, Education and Development of Unmanned Aerial Systems (RED-UAS). IEEE, 222-227.
- [12] Srikanth M, Annaswamy A, Lavretsky E (2010). Dynamic modeling and control of a flexible four-rotor UAV[C]//AIAA Guidance, Navigation, and Control Conference, 8050.
- [13] Shuai Heng (2016). Design And Implementation Of Micro Deformable Quadrotor [D]. Harbin Institute of Technology.
- [14] HOVAKIMYAN N C C. Adaptive Control Theory: Guaranteed Robustness with Fast Adaptation[M].
- [15] WANG J, CAO C, HOVAKIMYAN N (2008). L1 Adaptive Controller for a Missile Longitudinal Autopilot Design[J]. AIAA Guidance, Navigation and Control Conference and Exhibit, 2008(August):1-21.